Antiviral Research 162 (2019) 79–89

Contents lists available at ScienceDirect

Antiviral Research

journal homepage: www.elsevier.com/locate/antiviral

Metal chelators for the inhibition of the lymphocytic choriomeningitis virus endonuclease domain

Magali Saez-Ayala[a,e], Elsie Laban Yekwa[a,f], Clémence Mondielli[a], Loic Roux[a,g], Sergio Hernández[a], Fabrice Bailly[b], Philippe Cotelle[b,c], Dominga Rogolino[d], Bruno Canard[a], François Ferron[a], Karine Alvarez[a,*]

[a] Aix-Marseille Université, CNRS UMR 7257, Architecture et Fonction des Macromolécules Biologiques, 163 avenue de Luminy, 13288, Marseille, France
[b] Univ. Lille, Inserm, CHU Lille, UMR-S 1172 – JPArc - Centre de Recherche Jean-Pierre Aubert Neurosciences et Cancer, F-59000, Lille, France
[c] ENSCL, F-59000, Lille, France
[d] Dipartimento di Scienze Chimiche, della Vita e della Sostenibilità Ambientale, Università di Parma, Parma, P.co Area delle Scienze 17/A, Parma, Italy
[e] Aix-Marseille Université, CRCM, INSERM U1068, CNRS UMR7258, 13273, Marseille, France
[f] Division of Medical Virology, Faculty of Medicine and Health Sciences, Stellenbosch University, Tygerberg, South Africa
[g] Department of Physiology Anatomy and Genetics, Oxford University, Oxford, UK

ARTICLE INFO

Keywords:
Arenavirus
Metal chelators
LCMV
Endonuclease domain
Diketo acids
Polyphenols
N-Hydroxyisoquinoline-1,3-diones

ABSTRACT

Arenaviridae is a viral family whose members are associated with rodent-transmitted infections to humans responsible of severe diseases. The current lack of a vaccine and limited therapeutic options make the development of efficacious drugs of high priority. The cap-snatching mechanism of transcription of Arenavirus performed by the endonuclease domain of the L-protein is unique and essential, so we developed a drug design program targeting the endonuclease activity of the prototypic Lymphocytic ChorioMeningitis Virus. Since the endonuclease activity is metal ion dependent, we designed a library of compounds bearing chelating motifs (diketo acids, polyphenols, and *N*-hydroxyisoquinoline-1,3-diones) able to block the catalytic center through the chelation of the critical metal ions, resulting in a functional impairment. We pre-screened 59 compounds by Differential Scanning Fluorimetry. Then, we characterized the binding affinity by Microscale Thermophoresis and evaluated selected compounds in *in vitro* and *in cellula* assays. We found several potent binders and inhibitors of the endonuclease activity. This study validates the proof of concept that the endonuclease domain of Arenavirus can be used as a target for anti-arena-viral drug discovery and that both diketo acids and *N*-hydroxyisoquinoline-1,3-diones can be considered further as potential metal-chelating pharmacophores.

1. Introduction

The Lymphocytis Choriomeningitis Virus (LCMV) belongs to the *Arenaviridae* (Jay et al., 2005), a viral family whose members are associated with rodent-transmitted diseases in humans. *Arenaviridae* encompasses 5 viruses classified in the Category A Pathogen List (Borio et al., 2002) responsible for causing severe hemorrhagic fever. Lassa Fever virus, affects 2–3 million people annually in West Africa and induces between 15 and 30% mortality among hospitalized patients suffering from hemorrhagic fever. LCMV is the worldwide prototypic virus of the family. LCMV reservoir is the domestic mouse (*Mus musculus*) and occasional transmission to human occurs by contact with aerosols of fresh urine, droppings, saliva, nesting materials from infected rodents. The resulting infection can lead to life-threatening meningitis but it is mainly responsible for causing central nervous system disease, congenital malformation, choriomeningitis, all often leading to miscarriage (Barton and Hyndman, 2000). Several clinical studies point out that LCMV pathogenesis is underestimated (Bonthius, 2009).

The global weather and climate change (Clegg, 2009), may put 50 millions people at risk by 2020 in the region between Accra and the Niger delta. The recent outbreak of Lassa Fever virus in 2018 in Niger region reinforces the trends observed with an increase in virulence, an expansion of the areas of dissemination and the number of cases. Moreover, several new endemic areas have been reported, as well as more and more cases of imported arenavirus infections in Europe and the US.

Despite the global threat to human health, the biology of these

* Corresponding author. AFMB, Case 932, 163 avenue de Luminy, 13288 Marseille Cedex 9, France.
E-mail address: karine.alvarez@afmb.univ-mrs.fr (K. Alvarez).

https://doi.org/10.1016/j.antiviral.2018.12.008
Received 25 May 2018; Received in revised form 3 December 2018; Accepted 10 December 2018
Available online 14 December 2018
0166-3542/

viruses is still poorly understood, limiting therapeutic options to the use of the broad-spectrum antiviral ribavirin. Unfortunately, ribavirin displays mixed success in treating severe arenaviral disease and it is associated with significant toxicity (McCormick et al., 1986). This situation makes the development of efficacious drugs or vaccine of high priority. Even if the literature reporting anti-arenavirals (Pasquato and Kunz, 2016; Sepulveda et al., 2018) and vaccine development (Martinez-Sobrido and De la Torre, 2017) is scarce, there is a growing activity in the field (Bolken et al., 2006; Castilla et al., 2005; Uckun et al., 2005) targeting crucial steps of viral cycle such as entry (Chou et al., 2016; Larson et al., 2008; Ngo et al., 2016), replication (Mendenhall et al., 2011a, 2011b; Ortiz-Riano et al., 2014; Sepulveda et al., 2008, 2012) or maturation (Dai et al., 2013; Pasquato et al., 2012). Viral replication occurs in the cytoplasm of the infected cells and transcription is tightly coupled to translation. Arenaviruses encode an endonuclease domain (EndoN), located in the N-terminal region of the polymerase (Morin et al., 2010) and in charge of a “cap snatching” mechanism corresponding to the first step of viral transcription. This mechanism involves the recognition of capped cellular mRNAs and its subsequent cleavage (4–5 nucleotides downstream) to provide the RNA dependent RNA polymerase with a primer for viral transcription (Polyak et al., 1995a,b).

The cap-snatching mechanism currently known to be specific to *Arenaviridae, Orthomyxoviridae* and *Bunyavirales* is essential for viral transcription, thus making the endonuclease activity a good target for antiviral drug development. Main reasons are that (i) its inhibition could directly stall viral replication at the primary transcription step, (ii) the relevant active sites are likely to be highly conserved across strains and (iii) the viral endonuclease is divergent from human endoribonucleases.

We recently published the first crystal structures of an Arenavirus endonuclease domain in complex with two diketo acids (DKA), making them potent starting point for rational drug-design optimization (Saez-Ayala et al., 2018). However, because the EndoN active site is quite open, improving inhibitors using ligand-bound structures is a challenge. So, we decided to use a focused screening approach as an alternative strategy to discover potent inhibitors. Since the endonuclease activity is metal-dependent, chelation represents a relevant strategy to develop new inhibitors. The latter could efficiently coordinate the metal ions within the active site, preventing the interaction with the RNA substrate resulting in a functional impairment.

We rationally built a library comprising 59 molecules belonging to three main families: diketo acids (DKA), polyphenols (POP), and *N*-hydroxyisoquinoline-1,3-diones (HID) and complemented with some tetracyclines, chalcones, benzophenones and salicylamides. Despite their structural diversity, these compounds share a chelating motif able to contemporary coordinate metal ions. We pre-screened this library towards LCMV EndoN using Differential Scanning Fluorimetry and then characterized their binding affinity using Microscale Thermophoresis. Finally, we evaluated their efficacy in an *in vitro* endonuclease assay and in LCMV minigenome assay and infected cell cultures.

2. Materials and methods

2.1. Chemistry

Compounds **1**, **24**, **25**, **36** and **44** were purchased from Sigma-Aldrich. Compounds **2**, **3** and **4** were purchased from Fluka. Compound **8** was purchased from Interchim. Compound **37–40**, **42** and **56** were purchased from Alfa Aesar. Compounds **41** and **43** were purchased from Extrasynthese. Compounds **11**, **17**, **19** and **34** were purchased from Akos. Compounds **5, 6** and **35** were collected from the in-house library of AFMB laboratory (PCML, Plate-forme de criblage de Marseille Luminy). Compounds **9**, **12–16**, **20**, **21**, provided by F. Bailly and P. Cotelle, were synthesized according to previously reported methods (Drakulic et al., 2009; Maurin et al., 2004, 2006). Compounds **46–55**, provided by F. Bailly and P. Cotelle, were synthesized according to previously reported methods (Billamboz et al., 2011a, 2011b, 2013, 2016; Suchaud et al., 2014). Compounds **26**, **31**, **32**, **33**, provided by M. Carcelli and D. Rogolino, were synthesized according to previously reported methods (Sechi et al., 2006; Stevaert et al., 2015). Compound **45** provided by M. Carcelli and D. Rogolino, was obtained by modified literature procedure (Billamboz et al., 2008). Compounds **57–59**, provided by M. Carcelli and D. Rogolino, were synthesized according to previously reported methods (Carcelli et al., 2014, 2017). Compounds **7**, **10**, **18**, **22–23**, **27–30** were synthesized as described in the literature (Bhatt et al., 2011; Drakulic et al., 2009; Patil et al., 2007; Saez-Ayala et al., 2018; Verbic et al., 2007; Xu et al., 2006).

2.2. Enzyme production

The LCMV endonuclease (EndoN) wild type (EndoN-WT) and D118A and D88A mutants (EndoN-D118A and EndoN-D88A) were produced according to previously reported methods (Saez-Ayala et al., 2018). *Dictyostelium* nucleoside 5′-diphosphate kinase (NDPK) was obtained as previously described (Priet et al., 2015).

2.3. Differential Scanning Fluorimetry (DSF)

Melting temperature (T_m) values of proteins were determined by a thermo-fluorescence based assay (Koshland, 1958; Pantoliano et al., 2001). In 96-well thin-wall PCR plates, 11 µl of protein (EndoN) were added to 11 µl of compound solubilized in DMSO (5% DMSO final concentration), in 10 mM HEPES buffer, pH 8.0, 50 mM NaCl, 1 mM of $MgCl_2$, 1 mM of $MnCl_2$, and 2 mM DTT. Finally, 3 µl of the fluorescent dye Sypro Orange was added (Molecular Probes, 715-fold diluted in H_2O). Thermal denaturation of the proteins was followed by measuring fluorescence emission at 575 nm (with excitation at 490 nm) in a CFX Connect Real-Time PCR Detection System (Biorad) from 20 to 90 °C with increments of 0.2 °C. Final concentrations were adjusted to 75 µM of protein, 440 µM of $MgCl_2$, 440 µM of $MnCl_2$, 220 or 440 µM of compound (final ligand/protein ratio = 3 or 6), and 5% DMSO. Some representative melting curves obtained by DSF were presented in Fig. S5 - Supplementary data. compounds did not autofluoresce. Denaturation midpoints of proteins were calculated using the Boltzmann equation using GraphPad Prism. All measurements were performed in triplicates.

2.4. Microscale Thermophoresis (MST)

MST experiments with labelled (EndoN-WT, EndoN-D118A, EndoN-D88A, NDPK) proteins were performed on a Monolith NT.115 instrument (NanoTemper Technologies) as previously described (Saez-Ayala et al., 2018). NDPK was used as control to study specificity of measured interactions. K_D values were determined using the NanoTemper analysis software. Data were analyzed using MST or initial fluorescence (photobleaching rate). It was verified that the compounds did not cause autofluorescence (see Fig. S6A and S6B – Supplementary data). Some Curves are illustrated as examples in Fig. S7A, S7B, S8C, S8D and S9E – Supplementary data.

To study the influence of the experimental conditions on the binding efficiency, buffer nature and pH (10 mM HEPES buffers (pH 6, 7, 7.5 or 8) or in 10 mM TRIS buffers (pH 8, 9 or 10) containing 100 mM NaCl, 1 mM DTT, 0.05% (w/v) Tween-20, 0.25 mM $MgCl_2$ and 0.25 mM $MnCl_2$), metal ion nature (2 mM solutions of $MgCl_2$ and $MnCl_2$, or Mg $(SO_4)_2$ and $Mn(SO_4)_2$ or $Mg(NO_3)_2$ and $Mn(NO_3)2$) and metal ion concentration (equimolar solutions of $MgCl_2$ and $MnCl_2$ in a range of 0.002 mM to 10 mM) were varied.

2.5. Affinity of EndoN for RNA substrate by fluorescence polarization (FP)

Fluorescence polarization (FP) experiments were performed in

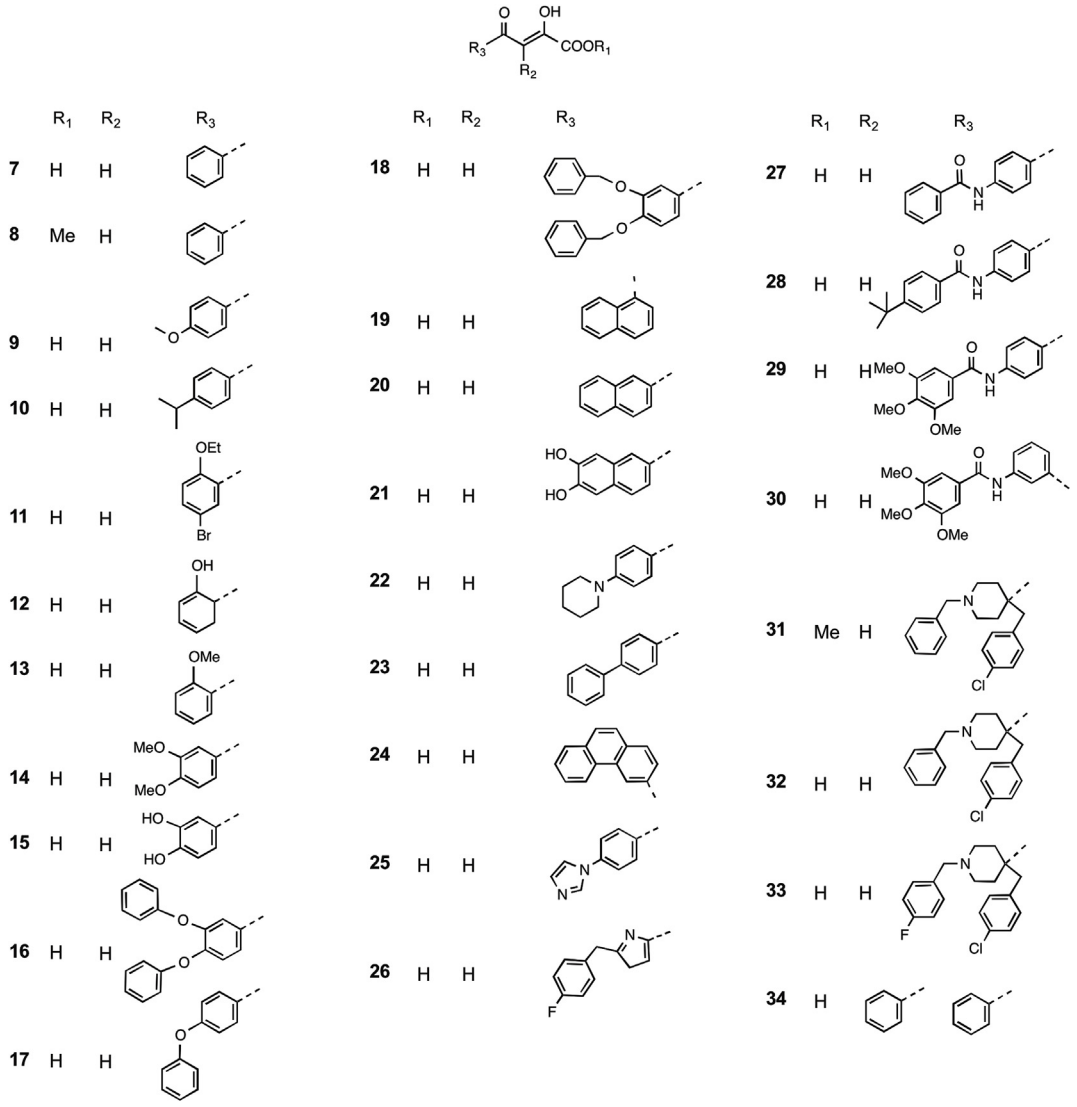

Fig. 1. Structure of DKA compounds family (**7**–**34**).

opaque black microtiter 96-well plates (Corning, Cat.No 3686) containing buffer (20 mM HEPES, pH 8.0, 50 mM NaCl, 2 mM DTT, 2 mM $MnCl_2$ or $MgCl_2$), 10 nM RNA template 5″-6-FAM-GUCCACGUAGACU AACAACU-3″ and increasing concentrations of proteins (0–300 μM). FP values were measured after 10 min at 520 nm (with excitation at 485 nm) on a microplate reader (PHERAstar FS, BMG Labtech). K_D values were calculated using the one-site specific binding equation with Hill slope, ($Y = B_{max} * Xh/(K_D h + Xh)$) using the GraphPad Prism software; where Y = FP change values, B_{max} = maximal FP change, X = protein concentration, h = Hill coefficient, and K_D = apparent equilibrium dissociation constant for RNA binding.

2.6. In vitro LCMV endonuclease assay

To investigate the inhibition of compounds **8**, **10**, **22**, **23**, **29** and **32** (DKA), **39** (POP), **46** and **52** (HID), *in vitro* endonuclease assays were performed as previously described (Saez-Ayala et al., 2018).

2.7. LCMV minireplicon activity and virus replication

Baby hamster kidney (BHK-21) cells and African green monkey kidney (VERO) cells were maintained in DMEM 1% GlutaMAX supplemented with 10% FBS (Thermo Fisher). All cell lines were grown at 37 °C in a humidified incubator containing 5% CO_2. For the minigenome assay, BHK-21 cells were co-transfected using 2.5 μl of Lipofectamine 2000 (Invitrogen) per μg of plasmids in 96 well plates with plasmids expressing LCMV NP (100ng/well) and L (125 ng/well) proteins and the minigenome (100 ng/well). The plasmid expressing the minigenome was kindly provided by Dr J.C. De La Torre and expressed a LCMV S segment where the viral genes GPC and NP were replaced by *Gaussia* Luciferase and eGFP genes, respectively. Five hours post-transfection, cell supernatants were removed and replaced by fresh medium containing the tested molecules at indicated concentrations. All tested molecules, including ribavirin (Sigma) were diluted in DMEM 1% GlutaMAX supplemented with 2% FBS and 1% DMSO (Thermoscientific). Reporter gene expression was monitored 3 days post-transfection either using an inverted fluorescence microscope or with the *Gaussia* luciferase assay kit (New England Biolabs). BHK-21 cells viability for each molecule concentration was assayed using PrestoBlue Cell Viability Reagent (Invitrogen). Molecules inhibiting minigenome were then tested in infected BHK-21 cells (Armstrong strain, multiplicity of infection (M.O.I) of 0.01). The spread of the virus through the cell monolayer was visualized using immunofluorescence and the viral titers were determined by end-point dilution assay on VERO cells and the Reed-Müench calculation method. Cells were fixed with 4% paraformaldehyde for 30 min followed by a permeabilization

treatment with 0.3% Triton X-100 (Merck), 3% Bovine Serum Albumin (Sigma) and 10% FBS in 1X PBS for 1 hour. Cells were stained with a mouse monoclonal antibody directed at LCMV NP, and a secondary goat anti-mouse Alexa Fluor 594 antibody (Thermo Fisher). All experiments were done in triplicate.

3. Results

3.1. Library design

The metal-chelation strategy to inhibit viral enzyme activity was explored to design inhibitors of influenza virus endonuclease, HIV RNAse H and integrase or HCV polymerase (Ju et al., 2017; Rogolino et al., 2012), and led to clinical developments. Raltegravir (Summa et al., 2008) and Dolutegravir (Kawasuji et al., 2013), two HIV integrase inhibitors, were approved respectively in 2007 and 2013. In 2018, Baloxavir marboxil, targeting influenza endonuclease activity was approved in Japan and Taïwan (Omoto et al., 2018) and more recently in US.

The first class of chelating inhibitors developed to target influenza endonuclease comprised 4-substituted-2,4-dioxobutanoic acids (Tomassini et al., 1994, 1996) with a characteristic β-diketo acid (DKA) motif. Among this series, the L742001 (**32**, Fig. 1) was identified as a potent inhibitor, both in enzyme- and cell-based antiviral assays (Hastings et al., 1996; Nakazawa et al., 2008; Stevaert et al., 2013; Song et al., 2016). Other classes of inhibitors have been reported (Rogolino et al., 2012; Stevaert et al., 2015). Interestingly, in the DKA series, the 2,4-dioxo-4-phenylbutanoic acid - DPBA (**8**, Fig. 1) was identified as inhibitor of the bunyavirus endonuclease (Reguera et al., 2010, 2016). Moreover, both were identified as binders to the LCMV endonuclease trough metal ion chelation (Saez-Ayala et al., 2018). Since the phenyl DKA **8** represents a suitable core to explore structure-activity relationships, several other DKAs (**7–34**, Fig. 1) with substituted phenyl rings (**23–25**, **27–30, 34**), polyaromatic naphthalene (**19–21**) and phenanthrene (**22**), heterocyclic rings (**26**) and, piperidine rings (**31–33**) were selected. We also put in polyphenols (POP) (**35–44**, Fig. 2). Epigallocathecin gallate **44** (EGCG) was found to be a potent inhibitor of influenza virus endonuclease (Kowalinski et al., 2012; Kuzuhara et al., 2009; Steinmann et al., 2013; Stevaert et al., 2013). This series of POP comprises flavones and flavonols substituted on the phenyl ring or on the chromone motif by hydroxyl or methoxy groups.

A series of *N*-hydroxyisoquinoline-1,3-diones (HID) (**45–56**, Fig. 3) was gathered in the library. The HIDs were originally designed as inhibitors of influenza virus endonuclease (Parkes et al., 2003), HIV integrase and RNaseH (Billamboz et al., 2008, 2011a, 2011b, 2013, 2016). More recently HIDs were evaluated against the HCV polymerase (Chen et al., 2012) and HBV RNase H (Cai et al., 2014; Edwards et al., 2017). We also included original scaffolds, such as tetracyclines, (**1–3**), chalcones and benzophenones (**4–6**, Fig. S3 – Supplementary data) and salicyl amides (**57–59,** Fig. S4 – Supplementary data) originally designed as HIV integrase and influenza endonuclease inhibitors (Agrawal et al., 2012; Carcelli et al., 2014, 2017).

To summarise, all compounds were selected on the basis of the metal chelation approach. Several substitution patterns were chosen on the chelating scaffolds, in order to explore electronic, structural and steric features critical for the binding process.

3.2. Pre-screening of the chelators library by DSF

Differential scanning fluorimetry (DSF) quantifies the change in thermal denaturation temperature of a protein under varying conditions. Since the binding of a ligand can increase the thermal stability of a protein (Koshland, 1958), DSF has been extensively used in drug screening campaigns (Cummings et al., 2006; Lo et al., 2004; Niesens et al., 2007; Pantoliano et al., 2001). Protein stability was studied in the presence or absence of metal cofactors and ligands, results are reported in Fig. 4.

The thermal melting transition for LCMV EndoN was observed at 38 °C in the absence of cofactor or ligand but was increased to 46 °C in the presence of the metal ions cofactors Mn^{2+} and Mg^{2+} and 5% DMSO. This melting temperature was used as a reference. The ligands were tested at 2 concentrations (220 µM and 440 µM, ligand/protein ratios of 3 and 6, respectively). Mostly, no significant difference was observed between the two concentrations, indicating that the lower ligand concentration was already sufficient to mediate a maximum effect on protein stabilization.

Tetracyclines **1–3** and chalcone **4** did not modify the thermal melting transition at 220 µM, highlighting the absence of interaction with EndoN. The precipitation of tetracycline **1** at 440 µM was responsible of drastic protein destabilization. Benzophenones **5** and **6** exhibited opposite behavior, by increasing and decreasing the melting temperature of 3 °C, respectively. DKAs (compounds **8** to **34**), induced a high protein stabilization with a ΔT_m from 4 to 17 °C, except for compounds **12** and **34**, for which weak destabilization was detected. POPs (compounds **35** to **44**) exhibited mixed behaviors. Compounds **34**, **35**, **40**, **42** and **44** induced moderate to drastic protein destabilization (ΔT_m from −3 to −10 °C), sometimes with a T_m value below the value of the native protein. Compounds **36** to **38** did not modify the thermal melting transition and compounds **39** and **43** induced moderate protein stabilization (ΔT_m 3 °C). Some HIDs (compounds **46** to **53**) induced moderate to drastic stabilization with a ΔT_m from 2 to 9 °C, whereas compounds **54** to **56** had no effect on protein stability or induced weak destabilization.

Therefore, major DKAs and HIDs are EndoN stabilizers by inducing an increase in the melting temperature, as a consequence of a binding interaction. Conversely major POPs are mostly destabilizers. Therefore, we decided to focus essentially on compounds that evidenced a stabilization effect towards the protein.

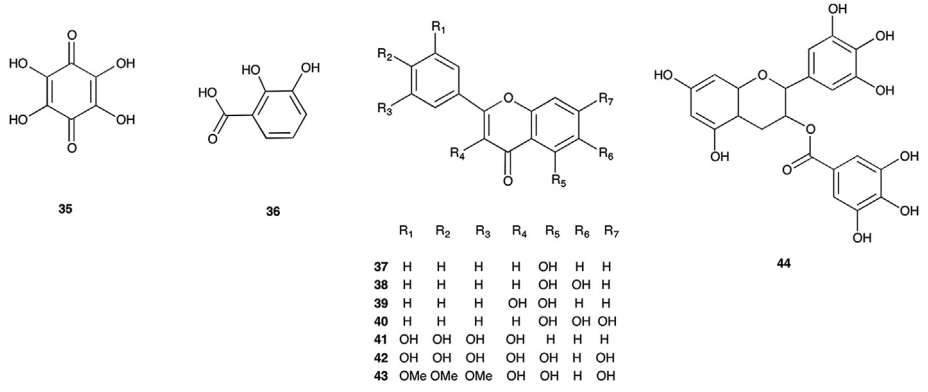

Fig. 2. Structure of POP compounds family (**35–44**).

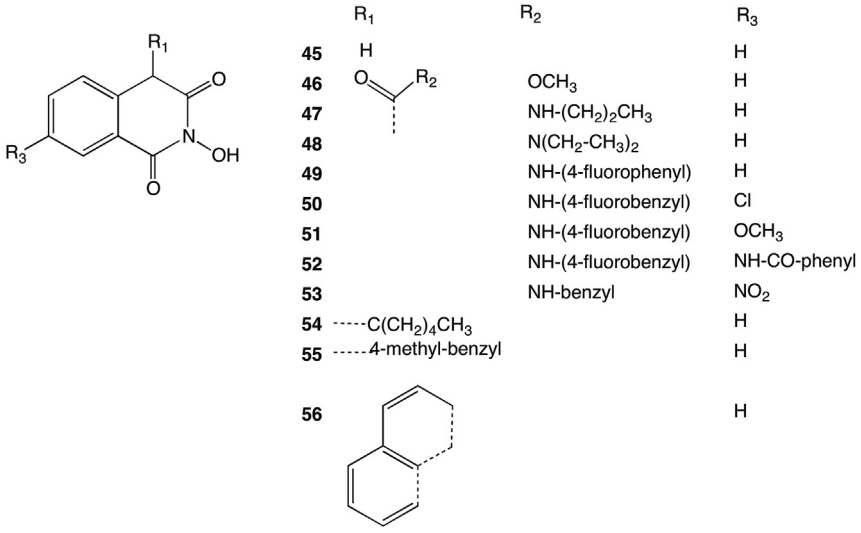

Fig. 3. Structure of HID compounds family (**45–56**).

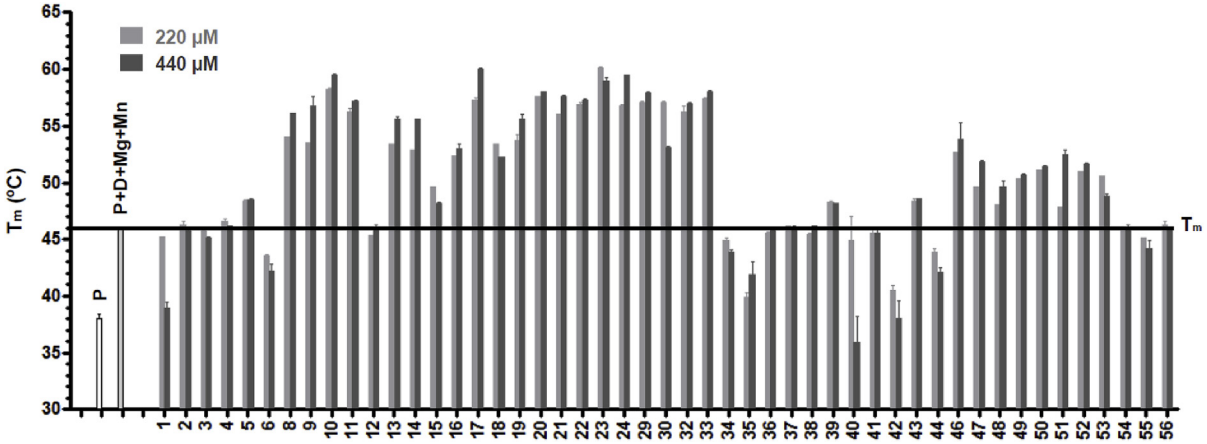

Fig. 4. (a) Thermal stability of LCMV EndoN determined by Differential Scanning Fluorimetry. The melting temperature (T_m) of EndoN (75 µM) (P), with the indicated divalent cation (0.5 mM) and 5% DMSO (P + D + Mg + Mn), or the compounds **1** to **56** (220 or 440 µM, ligand/protein ratio = 3 or 6) in presence of divalent cations (0.5 mM) and 5% DMSO, was measured in a Thermofluorescence experiment. Compounds **1** to **3**: tetracyclines. Compounds **4** to **6**: chalcone and benzophenones. Compounds **8** to **34**: diketo acid (DKA). Compounds **35** to **44**: polyphenol (POP). Compounds **45** to **56**: *N*-hydroxyisoquinoline-1,3-dione (HID).

3.3. Optimization of MicroScale thermophoresis (MST) conditions

MST uses the thermophoretic movement of the biomolecules in the presence or absence of cofactors and ligands to determine binding affinities. We first optimized experimental conditions regarding the effect of the buffer pH, the nature and concentration of the metal ions. The binding efficiency of EndoN-WT to DKA **8** did not change between pH 7.6 and 9 (≈5 µM) but was drastically reduced at lower pHs; pH 8.0 was selected as optimal pH.

The LCMV EndoN active site exhibits a narrow specificity for divalent metal ions (Mn^{2+} or Mg^{2+}) to catalyze RNA hydrolysis (Morin et al., 2010) and its activity is higher with Mn^{2+} than Mg^{2+}. Since the binding of DKAs and HIDs is mediated by metal ions chelation and because the nature of the metal cofactor influences the ligand binding, equimolar solutions of $MgCl_2$ and $MnCl_2$ in a range of 0.002 mM–10 mM were used in the assays. The optimal concentration was fixed at 0.5 mM as no noticeable change was observed at lower concentrations and precipitation of EndoN-WT was observed at higher concentrations (5–10 mM). We measured and compared the dissociation constants for DKAs **8** and **32**, and HID **50** with Mn^{2+} or Mg^{2+} or a mixture of Mn^{2+}/Mg^{2+}. For both families, the affinity was similar with Mn^{2+} and with the mixture Mn^{2+}/Mg^{2+}, but was slightly lower with Mg^{2+} (3- to 6-fold lower). These results confirm that the nature of metal ion cofactor may influence the ligand binding efficiency as a consequence of the different hard/soft nature of the Lewis acid (Bacchi et al., 2011).

To sum up, experimental conditions were optimized taking into account the factors influencing protein binding *i.e.* the buffer pH and the nature and concentration of metal ions, since the other variables considered did not influence the protein-compound interaction.

3.4. Ligand binding affinity determination using MST

3.4.1. Diketo acids (DKA)

Results are gathered in Table 1. EndoN-WT displayed potent affinity for most DKAs, except for 5 compounds. For the reference phenyl DKA **8**, a K_D value of 5.38 µM was measured. Interaction with EndoN-WT was completely lost in absence of metal ions (Fig. S7A – Supplementary data), indicating that the binding is mediated by metal ions chelation. Phenyl DKAs are di-acids, at pH 8 the relevant species is the mono-deprotonated form which complexes with the metal ions. Interaction is specific to EndoN since *Dictyostelium* nucleoside 5′-diphosphate kinase (NDPK) did not show any affinity for DKA **8** (see Fig. S7A and S7B – Supplementary data).

The absence of binding of phenyl diketo ester (DKE) **7**, phenyl DKA **12** and piperidinyl DKE **31** is due to their inability to chelate divalent

Table 1
Binding affinities of diketo acids (DKA) **7** to **34** determined by MST. The concentration of labelled protein EndoN-WT was kept constant at 100 nM, while the concentration of compound was varied from 500 μM or 250 μM in a 15-step two-fold dilution series. MST was measured with 80% LED power and 80% infra-red laser power. K_D values were determined using the NanoTemper analysis software (MST data). *: published results (Saez-Ayala et al., 2018).

Compound	K_D (μM)
7	> 250
8	5.38 ± 2.06*
9	4.34 ± 0.45
10	0.25 ± 0.12
11	1.52 ± 0.22
12	> 250
13	6.24 ± 0.15
14	2.48 ± 0.74
15	2.38 ± 0.37
16	0.39 ± 0.30
17	0.39 ± 0.14
18	0.32 ± 0.16
19	3.19 ± 0.96
20	0.35 ± 0.02
21	0.28 ± 0.01
22	0.25 ± 0.07*
23	0.05 ± 0.02*
24	0.11 ± 0.03
25	1.23 ± 0.57
26	0.83 ± 0.12
27	0.22 ± 0.14
28	0.48 ± 0.16
29	0.16 ± 0.05
30	> 250
31	> 250
32	0.51 ± 0.11*
33	0.89 ± 0.35
34	122.5 ± 7.70

metal ions. For DKEs **7** and **31**, this failure is due to their ester form. For phenyl DKA **12**, we reasoned that the hydrogen bond with the ortho-OH tautomeric equilibrium should enhance the pKa of the ligand which is not negatively charged and unable to complex metal ions. For DKAs **30** and **34**, the steric hindrance results in binding failure, in particular for compound **34** bearing a benzylidene group between the γ-ketone and the enolizable α-ketone.

Overall, phenyl DKAs **8** to **29** displayed affinity from sub-micromolar to micromolar level, but differences can be observed within the series, depending on the size and substitution of the aromatic ring. Compounds **16** to **18**, displayed 15-fold better affinity (≈0.30 μM) compared to the reference DKA **8**. We reasoned that introducing larger aromatic moieties on the phenyl ring could reinforce the binding by establishing hydrophobic contacts with residues of the active site in addition to affecting positively the acidic constant values. DKAs **20**, **23** and **24** bearing respectively naphtyl, bi-phenyl and phenantryl ring displayed K_D values of 0.35, 0.05 and 0.11 μM, showing 15- to 100-fold better affinities compared to the reference DKA **8**. The potent bi-phenyl derivative **23** allowed probably the second ring to rotate and establish additional interactions compared to **20** and **24**. On the other hand, the substitution of the second phenyl ring by an aromatic heterocycle type imidazole (compound **25**) improved the affinity only by a factor of 5. Compound **22** with a phenylpiperidine ring, a non-condensed bicyclic scaffold, displayed 50-fold better affinity compared to **8**. We hypothesized that the piperidine ring, protonated at pH 8, may interact with amino acids of the active site *via* electrostatic or hydrogen bonding. Overall, as expected, aromaticity, flexibility and the possibility to establish hydrogen bond of the aromatic part of the DKA scaffold seemed to drive ligand accommodation. We also evaluated a series of diversely substituted 4-benzamido-phenyl scaffold; compounds **27** to **29** displayed K_D values of 0.22, 0.48 and 0.16 μM, showing 20 to 30-fold better affinities compared to **8**. However, when the substituent was in meta-position on the phenyl ring (compound **30**), the binding efficiency was lost (K_D > 250 μM). The critical role of the ring orientation on ligand accommodation was confirmed by comparing compound **20** (β-ring) and **19** (α-ring), for wich binding efficiency was reduced by 10-fold.

We also evaluated ligands derived from DKA L742001 (**32**), known as a potent influenza virus endonuclease inhibitor (Stevaert et al., 2015), for which the β-diketo acid motif was linked to a piperidine moiety carrying two benzyl substituents. As expected, the DKE **31** was not a good binder, whereas the corresponding DKA **32** displays potent affinity (K_D value of 0.50 μM). We previously described (Saez-Ayala et al., 2018) that the two aromatic "wings" of the compound were crucial for achieving potent binding to LCMV EndoN, in addition to the divalent metal chelating pharmacophore.

In order to further investigate the mode of binding of the DKAs, the two mutants EndoN-D88A and EndoN-D118A were used to elucidate the role of the residues D88 and D118 in ligand binding. The D88A is a mutation on the supposed key residue involved in bivalent metal ion coordination, while the D118A is a mutation away from the active site of a conserved residue part of the catalytic pocket (Saez-Ayala et al., 2018). As expected, the affinity of EndoN-D88A for tested compounds **8**, **10**, **23**, and **32** was completely lost (See also Fig. S8D – Supplementary data). On the contrary, the affinity of EndoN-D118A for the same compounds was comparable with what we observed for the EndoN-WT, meaning that the residue D118 does not play a direct role in the binding of the DKAs.

All these results corroborated the idea that the binding of the DKA take place *via* the chelation of the divalent cations within the active site and that in addition to the chelating ability of the DKA scaffold (γ-ketone, enolizable α-ketone and carboxylic acid) the role of the substituents of the aromatic ring is critical to ensure optimal binding mode.

3.4.2. Polyphenols (POP)

Since most POPs destabilized EndoN, as shown by DSF experiments, we performed binding affinity measurements only on few compounds that were stabilizers or without effect. We evaluated compounds **36** to **39**, **41** and **43**. As expected, POPs were poor binders with K_D values of 67.70 ± 2.90 and 14.08 ± 4.22 μM for compounds **39** and **41**, respectively, or displayed no effect with K_D values > 250 μM for compounds **36** to **38** and **43**.

3.4.3. N-hydroxyisoquinoline-1,3-diones (HID)

Results are gathered in Table 2. Compound **45** was used as prototype of this family and displayed a K_D value of 2.17 μM. The introduction of an ester function or of an alkyl-carboxamide group on position 4 of the isoquinoline ring in compounds **46**, **47** and **48** leaded to a diminution of K_D values 2–5-fold respect to the reference ligand **45**. The introduction of a *N*-benzyl-carboxamide was also favorable for binding (compounds **50**–**53**) with similar K_D values and the best compound **51** displayed K_D value of 0.25 μM (9-fold better than **45**). However, a *N*-phenyl-carboxamide substituent (compound **49**) was unfavorable, (9-fold lesser than **45**); this could be related to differences in flexibility between *N*-benzyl- and *N*-phenyl, with probably a better accommodation of the phenyl ring in the *N*-benzyl-compound towards an aromatic residue of the catalytic site. The introduction of alkyl or aromatic moieties at position 4 of the hydroxyisoquinoline dione moiety was completely defavorable, since no binding was observed for compounds **54** to **56**.

In analogy with DKA, we tested compound **50** (Fig. S7B – Supplementary data), also in absence of metal ions and with the mutant D88A. Results showed that affinity was completely lost in both cases, underlying again that the binding of HID is mediated by metal ions chelation.

Table 2
Binding affinities of *N*-hydroxyisoquinoline-1,3-diones (HID) **45** to **56** determined by MST. The concentration of labelled protein was kept constant at 100 nM, while the concentration of compound was varied from 500 µM or 250 µM in a 15-step two-fold dilution series. After 5 min incubation period the MST was measured with 80% LED power and 80% infra-red laser power. K_D values were determined using the NanoTemper analysis software (initial fluorescence – photobleaching rate).

Compound	K_D (µM)
45	2.17 ± 0.80
46	0.40 ± 0.04
47	0.81 ± 0.03
48	0.79 ± 0.16
49	9.67 ± 2.11
50	1.24 ± 0.70
51	0.25 ± 0.01
52	0.75 ± 0.06
53	0.80 ± 0.20
54	> 250
55	ND
56	> 250

3.4.4. Tetracyclines, chalcones, benzophenones and salicyl amides

Chalcone **4** displayed any affinity for EndoN until 250 µM and benzophenone **5** displayed weak affinity (K_D value of 74.75 ± 4.76 µM). Salicyl amides (**57**–**59**) were originally designed as HIV integrase and influenza virus endonuclease inhibitors. Any tested salicyl amides displayed no affinity for EndoN up to 250 µM.

3.5. Correlation between DSF and MST data

In order to validate the pre-screening of our compounds library, we performed correlation of the thermal melting transition values and affinity measurement. Results are illustrated in Fig. S10 – Supplementary data. Thermal stability and affinity were strongly correlated for DKAs with linear coefficient r of −0.72. For DKAs, the smaller the K_D value, the greater the effect on the T_m, meaning that induced stabilization of protein was positively related to the ligand affinity (ΔTm from 4 to 17 °C). For HIDs, a direct correlation between protein thermal stability and binding affinity was not observed. Indeed, the thermal stability was almost identical (ΔT_m from 2 to 8 °C) irrespective of the affinity.

3.6. Metal ion preference of the EndoN for RNA binding

In order to develop EndoN activity assay, we performed the titration of an RNA substrate model by fluorescence polarization by increasing concentration of EndoN in the presence of Mn^{2+} or Mg^{2+} (Fig. S11 – Supplementary data) or a mixture of Mn^{2+}/Mg^{2+} (data not shown). The affinity of the EndoN-WT for RNA substrate with Mn^{2+} or a mixture of Mn^{2+}/Mg^{2+} was quite similar (K_D values of 29.9 ± 1.1 µM) but weak with Mg^{2+} making difficult to calculate reliable affinity value (K_D > 100 µM). In order to map the RNA binding, we performed also titration on mutants EndoN-D118A and EndoN-D88A. As expected, with the mutant D88A, RNA binding was lost, whatever the metal ion used. Conversely, the affinity of the EndoN-D118A mutant for RNA substrate was similar with Mn^{2+} and Mg^{2+} (K_D values ≈ 35 µM). This result indicates that side residue such as D118 does not have a direct effect on binding of the ligand to the active site *via* metal ion chelation but might guide the RNA towards the catalytic center.

As a whole, we herein showed that RNA bindings are mainly mediated in the active site through the metal ions trapping efficiency and preference (i.e. for Mn^{2+}) and consequently the capacity of the active site to accommodate catalytic ions and guide the RNA substrate.

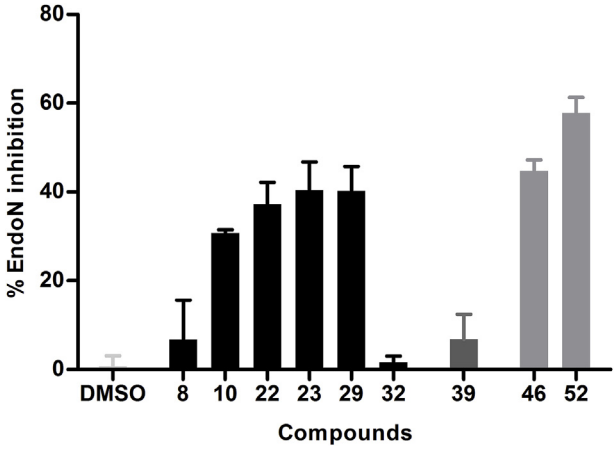

Fig. 5. Quantification of endonuclease activity inhibition in presence of 5% DMSO or compounds **8**, **10**, **22**, **23**, **29**, **32** (DKA), **39** (POP), **46** and **52** (HID). Results obtained with compound **8, 22, 23** and **32** were previously published (Saez-Ayala et al., 2018). Compounds at a final concentration of 50 µM with 5% DMSO were incubated with 20 µM of protein and 1 µM of single stranded RNA. After 6 h reaction at RT, the products were analyzed in 20% polyacrylamide/8M urea gels. The undigested RNAs were quantified by phosphoimager (Fuji) and graph was plotted using GraphPad PRISM. All experiments were performed in triplicates.

3.7. Inhibition of EndoN activity in a in vitro endonuclease assay

We tested the efficiency of compounds **8**, **10**, **22**, **23**, **29** and **32** (DKA) **39** (POP) **46** and **52** (HID) to inhibit the LCMV endonuclease activity in an *in vitro* endonuclease assay. The compounds were selected according to their availability, solubility and affinity. A 5′-radiolabelled RNA substrate model was incubated with the EndoN-WT and 50 µM of compound and RNA cleavage was analyzed on a denaturing polyacrylamide gel and visualized on a phosphoimager. Quantification results are shown in Fig. 5.

As previously reported (Saez-Ayala et al., 2018), phenyl DKA **8** and piperidinyl DKA **32** displayed weak inhibition of LCMV endonuclease activity at 50 µM, while ligands **22** and **23**, which bear respectively, biphenyl, and phenantryl moieties, displayed 35 and 40% inhibition at the same concentration. Ligands **10** and **29** (DKAs) with a para-isopropylphenyl and a benzamidophenyl group, respectively displayed similar inhibitions (30–40%) at 50 µM. Except for compound **32**, high binding affinities seemed to be correlated with potent *in vitro* inhibitions of EndoN activity. Indeed, DKAs **10**, **22**, **23** and **29** displayed around 40% inhibition at 50 µM with K_D values ranging from 0.05 to 0.25 µM (Table 1).

DKA **29** displays moderate activity thanks to the flexible and large benzamido-phenyl scaffold, allowing the second ring to rotate and to establish additional contacts in the protein pocket. The smaller DKA **10** may act differently by formation of diketo tweezers: a complex involving two cations and two DKA ligand molecules. This type of tweezer has been described for DKAs and also for HIDs with Mn^{2+} ions specifically (Billamboz et al., 2011b). This constitutes an important question that should be addressed.

As we described previously, DKA **32** is fitted in the LCMV EndoN active site, essentially by metal chelation (Saez-Ayala et al., 2018). The lack of polar, hydrophobic or electrostatic interactions lead to residual flexibility and sub-optimal efficacy and makes DKA **32** potent ligand but weak inhibitor.

For POP, the compound **39** which is a poor binder (K_D = 67.70 µM) is also a weak inhibitor (8%).

For HID, compounds **46** and **52** are both good inhibitors (43 and 58%, respectively) and good binders (K_D of 0.40 and 0.75 µM, respectively, Table 2).

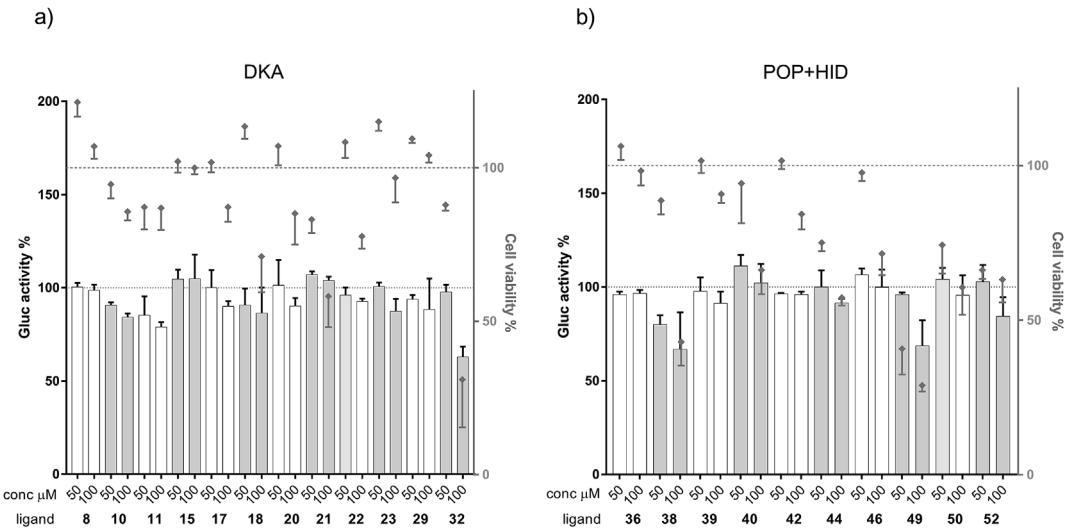

Fig. 6. Effect of DKAs (a) and POPs + HIDs (b) in the minigenome assay of LCMV (bars) and in cell viability (diamonds). BHK-21 cells in 96 well plates were transfected with the plasmids expressing the minigenome, and 5 hours post-transfection the culture supernatant was replaced with fresh media containing the indicated ligand. 3 days post-transfection luciferase activity was monitored in parallel with the cell viability. Each condition was done in triplicates.

3.8. Evaluation of compounds onto the LCMV minireplicon activity and virus replication

We proceeded to test the efficiency of the compounds **7**, **8**, **10**, **11**, **15**, **17**, **18**, **20–23**, **29**, **32** (DKA) **36**, **38**, **39**, (POP) **46**, **49**, **50**, **52** (HID) in a LCMV replicon assay.

Since the compounds were supposed to target the polymerase function, the assay was particularly suited to detect a decrease of the minigenome replication and/or transcription through the quantitative measurement of the GLuc reporter gene. We also tested the cytotoxic effect of the compounds (Fig. 6). Out of the 20 compounds, fourteen had no effect on the reporter gene expression whatever were the tested concentrations, whereas the positive controls resulted either in a 25% decrease (ribavirin at 50 µM) or a 66% decrease (ribavirin at 100 µM). 5 compounds presented a cytotoxic effect at the concentration associated with a decrease of GLuc expression. For compounds **32**, **49** and **52**, the cytotoxicity was very pronounced, associated with more than 50% cell death 3 days post-treatment. For compounds **10** and **11**, a moderate cytotoxicity was associated with a moderate inhibition (15–22%) of the minigenome expression. Compounds **18**, **29** and **38** presented at certain concentrations a moderate inhibition (until 14%) without cytotoxicity. Several compounds were then further studied to determine their effect on the growth of the LCMV. The BHK-21 cells were infected at a M.O.I. of 0.01 by the virus in the presence of the compounds. Three day post-infection, viral titers were determined. The ribavirin showed a very strong inhibition of the virus replication: a 5-log reduction on viral titer at 50 µM and titer below the limit of detection at 100 µM. Most of the compounds did not show any effect. Compounds **18** and **11**, which showed a moderate effect onto the GLuc expression did not show any inhibition on virus replication (Figs. S12 and S13 – Supplementary data). Compound **23** showed almost a 3-fold decrease of the viral titer at 50 µM. A second experiment was done with other combinations of compounds and concentrations (Fig. S13 – Supplementary data). None of the compounds had any detectable inhibitory effect on viral titers. Compounds **32** and **38** were tested in a last experiment at different time-points of the infection (Fig. 7). Compound **38** induced a 13-fold and a 2.4-fold decrease of the viral titer by day 1 and 2, respectively but by day three, the inhibitory effect was undetectable. Compound **32**, despite being cytotoxic onto the BHK-21 cells by day 3, had no detectable effect onto the cell viability by day 1 (Fig. S14 – Supplementary data). Compound **32** strongly inhibited the viral replication by day 1. Indeed, the viral titer was diminished by 3 logs and probably resulted only from what remained of the initial inoculum.

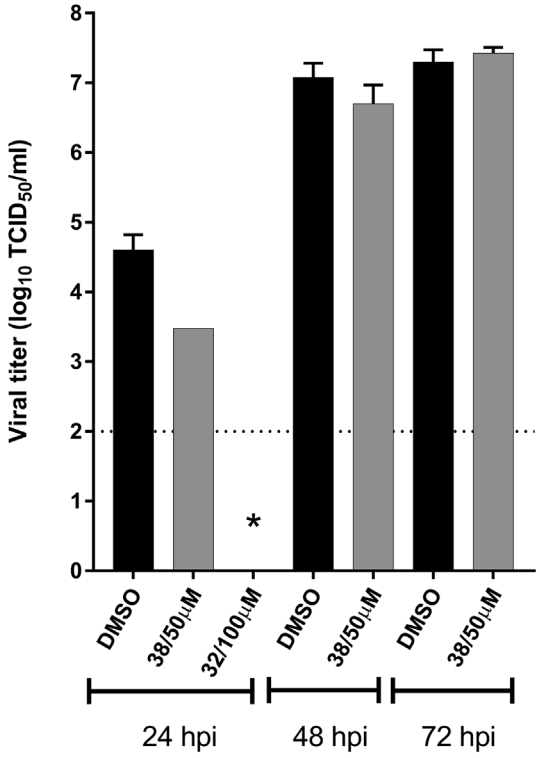

Fig. 7. Inhibitory effect of compounds **32** and **38** onto the LCMV. BHK-21 cells in 96 well plates were infected at a MOI of 0.01 and treated with indicated concentration of compounds. At indicated time points post-infection, the supernatants were collected and titrated. Each condition was done in triplicates. The dotted line represents the limit of detection of the titration assay. * indicates that the viral titer was close to the limit of detection.

4. Discussion

In order to design inhibitors of the LCMV EndoN, we followed a metal chelation approach. Our strategy was to find ligands able to block the catalytic center through the chelation of critical metal ions within the active site that would translate into a functional impairment.

We built a « chelators library » of 59 compounds, divided into 3 main families: DKAs, POPs and HIDs which were never tested against arenaviruses. Our library was first pre-screened on LCMV EndoN using DSF. Major ligand-induced protein stabilization was observed with DKAs, to a lesser extent with HIDs and strong destabilization was measured with POPs. In light of these results, DKAs and HIDs are considered as potent EndoN binders. Conversely POPs do not give a specific and reproducible interaction.

Next, we measured binding affinities by MST for all stabilizers. Apart from the compounds that did not show any binding, most DKAs and HIDs displayed affinities in the nanomolar to micromolar range. Binding was completely lost without metal ions and with the catalytic mutant D88A, indicating that is mainly mediated by metal ions chelation. For DKAs, a good correlation between thermal melting transition values and affinity was observed. The chelating motif of DKAs (γ-ketone, enolizable α-ketone and carboxylic acid) is strictly necessary and must be intact to ensure optimal binding mode. DKAs binding efficiency is deeply improved introducing large aromatic substituent on the phenyl ring which could establish hydrophobic contacts with residues of the active site. Moreover, the importance of the aromatic framework, by the way of its electronic influence on the α-diketo moiety, affects directly the acidic constant values, one of the most important parameters involved in DKA-ions complex formation (Sechi et al., 2006).

For HID, the chelation is ensured by the three oxygen triad of the *N*-hydroxyimide moiety. HID binding efficiency is dependent of the substituents on the position 4 of the isoquinoline ring. The introduction of alkyl, benzyl or naphthyl groups is unfavorable, in contrast to *N*-alkyl-(or *N*-benzyl)-carboxamides. It has been proposed that the carboxamide in position 4 impacts the resonance stabilization of the enolate required for metal chelation and is able to create an intramolecular hydrogen bond with the oxygen at position 3 also favorable for metal ion chelation (Billamboz et al., 2013). As described previously (Saez-Ayala et al., 2018), to be inhibitors of LCMV endonuclease activity, phenyl DKAs has to bear large aromatic moieties on the phenyl ring. Hence, their efficiency is related to their capacity to chelate metal ions and also establish hydrophobic interactions with some key amino acids of the active site. HIDs are also moderate inhibitors of LCMV endonuclease activity. The relative higher inhibition observed with HIDs compare to DKAs, could be explained by their supposed larger surface of interaction in the active site of the EndoN.

In conclusion, the anchorage of compound by metal chelation is necessary but not sufficient for efficacious inhibition: to design potent inhibitors, a combination of peculiar structural, steric, and electronic features of the substituents of the chelating scaffold has to be performed, in order to identify the features necessary to obtain good activity by fullest occupancy binding mode.

Regarding the efficiency of the compounds in a LCMV replicon assay and in LCMV infected cell cultures, amongst the 22 tested compounds, only DKA **32** and POP **38** slightly inhibited the virus growth, mostly at the beginning of the infection. Because POP **38** did not bind target EndoN, another function could be affected by the compound. In accordance with this assumption, POP **44** [EGCG] was previously described as inhibitor of influenza virus through alteration of physical integrity of virus particles, reduction of reactive oxygen species (ROS) or by inhibition of entry through binding to haemagglutinin (Imanishi et al., 2002; Ling et al., 2012; Nakayama et al., 1993; Song et al., 2005).

DKA **32** was originally identified as a potent inhibitor of influenza viral growth in both cell culture and mouse models (Hastings et al., 1996; Nakazawa et al., 2008; Parkes et al., 2003; Tomassini et al., 1994). This compound, more recently, was described to be able to reduce the accumulation of viral RNAs in PR8 influenza virus infected cells by inhibiting the RNA polymerase (Song et al., 2016). In our assays, DKA **32** showed a very strong inhibition of the viral load in LCMV infected cells by day 1 post-treatment (3 log), however its cytotoxicity in the sensitive BHK-21 cells by day 3 post-treatment prevented the observation of extended antiviral activity. We do not exclude that another cellular model less tenuous to the transfection or infection interference may help to understand the effect of DKA **32** and to identify the target of this compound, that could be another viral nuclease used by the virus to escape the immune system during infection (Reynard et al., 2014).

5. Conclusion

We assembled a focused library never screened before against the LCMV endonuclease domain, on the basis of a chelation strategy. We found several potent binders and inhibitors of its activity. Both diketo acids and *N*-hydroxyisoquinoline-1,3-diones can be considered now as anti-EndoN metal-chelating pharmacophores. Reporting specificities in the recognition properties of these compounds, these two pharmacophores make different contributions to their interaction with EndoN catalytic site and these differences should be taken into account for the improvement of their inhibitory properties. Interestingly, the tested compounds demonstrated moderate (DKA) to good (HID) inhibition at 50 μM in *in vitro* enzymatic assays, re-enforcing the idea that chelating ligands can be active across metal-dependent viral enzymes.

Unfortunately, in a sub-optimal cellular model, cytotoxicity impaired the cell-culture assays of the most interesting compounds and other resulted inactive, probably as a result of poor membrane permeability of ionic compounds as DKA and HID or low chemical stability or rapid metabolism.

Divalent cation chelators have already been FDA-approved for clinical use and success against several viral diseases. This validated the « metal chelation strategy » as an important milestone in drug design that could lead to the development of efficient inhibitors also in the case of Arenaviruses.

Funding

This work was supported by Agence Nationale pour la Recherche (ANR) grant ArenaBunya-L (ANR-11-BSV8-0019), the Fondation pour la Recherche Médicale (FRM) (SPF20130526788), the Fondation Méditerranée Infection, and the French Infrastructure for Integrated Structural Biology (FRISBI) (ANR-10-INSB-05-01).

Acknowledgements

The Authors thanks Dr Sébastien Emonet and Dr Christophe Peyrefitte (Unité de Virologie, Département de Biologie des Agents Transmissibles, IRBA, Brétigny-sur-Orge cedex, France) for doing all the experiments in cell cultures and for useful discussions. The Authors thanks Maria Maté-Perez, Julie Lichière, Barbara Selisko, Kévin Botelho Ferreira for their technical assistance, and Dr. Bruno Coutard, Dr. Juan Reguera, Dr Laurent Hoffer and Dr. Mauro Carcelli for useful discussions.

Appendix A. Supplementary data

Supplementary data to this article can be found online at https://doi.org/10.1016/j.antiviral.2018.12.008.

References

Agrawal, A., DeSoto, J., Fullagar, J.L., Maddali, K., Rostami, S., Richman, D.D., Pommier, Y., Cohen, S.M., 2012. Probing chelation motifs in HIV integrase inhibitors. Proc. Natl. Acad. Sci. U. S. A. 109, 2251–2256.

Bacchi, A., Carcelli, M., Compari, C., Fisicaro, E., Pala, N., Rispoli, G., Rogolino, D., Sanchez, T.W., Sechi, M., Sinisi, V., Neamati, N., 2011. Investigating the role of metal chelation in HIV-1 integrase strand transfer inhibitors. J. Med. Chem. 54, 8407–8420.

Barton, L.L., Hyndman, N.J., 2000. Lymphocytic choriomeningitis virus: reemerging central nervous system pathogen. Pediatrics 105, E35.

Bhatt, A., Gurukumar, K.R., Basu, A., Patel, M.R., Kaushik-Basu, N., Talele, T.T., 2011. Synthesis and SAR optimization of diketo acid pharmacophore for HCV NS5B polymerase inhibition. Eur. J. Med. Chem. 46, 5138–5145.

Billamboz, M., Bailly, F., Barreca, M.L., De Luca, L., Mouscadet, J.-F., Calmels, C., Andréola, M.-L., Witvrouw, M., Christ, F., Debyser, Z., Cotelle, P., 2008. Design, synthesis and biological evaluation of a series of 2-hydroxyisoquinoline-1,3(2H,4H)-diones as dual inhibitors of human immunodeficiency virus type 1 integrase and the reverse transcriptase RNase H domain. J. Med. Chem. 51, 7717–7730.
Billamboz, M., Bailly, F., Lion, C., Calmels, C., Andreola, M.L., Witvrouw, M., Christ, F., Debyser, Z., De Luca, L., Chimirri, A., Cotelle, P., 2011a. 2-hydroxyisoquinoline-1,3(2H,4H)-diones as inhibitors of HIV-1 integrase and reverse transcriptase RNase H domain: influence of the alkylation of position 4. Eur. J. Med. Chem. 46, 535–546.
Billamboz, M., Bailly, F., Lion, C., Touati, N., Vezin, H., Calmels, C., Andreola, M.L., Christ, F., Debyser, Z., Cotelle, P., 2011b. Magnesium chelating 2-hydroxyisoquinoline-1,3(2H,4H)-diones, as inhibitors of HIV-1 integrase and/or the HIV-1 reverse transcriptase ribonuclease H domain: discovery of a novel selective inhibitor of the ribonuclease H function. J. Med. Chem. 54, 1812–1824.
Billamboz, M., Suchaud, V., Bailly, F., Lion, C., Andreola, M.L., Christ, F., Debyser, Z., Cotelle, P., 2016. 2-hydroxyisoquinoline-1,3(2H,4H)-diones (HIDs) as human immunodeficiency virus type 1 integrase inhibitors: influence of the alkylcarboxamide substitution of position 4. Eur. J. Med. Chem. 117, 256–268.
Billamboz, M., Suchaud, V., Bailly, F., Lion, C., Demeulemeester, J., Calmels, C., Andreola, M.L., Christ, F., Debyser, Z., Cotelle, P., 2013. 4-Substituted 2-hydroxyisoquinoline-1,3(2H,4H)-diones as a novel class of HIV-1 integrase inhibitors. ACS Med. Chem. Lett. 4, 606–611.
Bolken, T.C., Laquerre, S., Zhang, Y., Bailey, T.R., Pevear, D.C., Kickner, S.S., Sperzel, L.E., Jones, K.F., Warren, T.K., Amanda Lund, S., Kirkwood-Watts, D.L., King, D.S., Shurtleff, A.C., Guttieri, M.C., Deng, Y., Bleam, M., Hruby, D.E., 2006. Identification and characterization of potent small molecule inhibitor of hemorrhagic fever New World arenaviruses. Antivir. Res. 69, 86–97.
Bonthius, D.J., 2009. Lymphocytic choriomeningitis virus: a prenatal and postnatal threat. Adv. Pediatr. 56, 75–86.
Borio, L., Inglesby, T., Peters, C.J., Schmaljohn, A.L., Hughes, J.M., Jahrling, P.B., Ksiazek, T., Johnson, K.M., Meyerhoff, A., O'Toole, T., Ascher, M.S., Bartlett, J., Breman, J.G., Eitzen Jr., E.M., Hamburg, M., Hauer, J., Henderson, D.A., Johnson, R.T., Kwik, G., Layton, M., Lillibridge, S., Nabel, G.J., Osterholm, M.T., Perl, T.M., Russell, P., Tonat, K., Working Group on Civilian, B., 2002. Hemorrhagic fever viruses as biological weapons: medical and public health management. JAMA 287, 2391–2405.
Cai, C.W., Lomonosova, E., Moran, E.A., Cheng, X., Patel, K.B., Bailly, F., Cotelle, P., Meyers, M.J., Tavis, J.E., 2014. Hepatitis B virus replication is blocked by a 2-hydroxyisoquinoline-1,3(2H,4H)-dione (HID) inhibitor of the viral ribonuclease H activity. Antivir. Res. 108, 48–55.
Carcelli, M., Fisicaro, E., Compari, C., Contardi, L., Rogolino, D., Solinas, C., Stevaert, A., Naesens, L., 2017. Metal-chelating properties and antiviral activity of some 2-hydroxyphenyl amides. Polyhedron 129, 97–104.
Carcelli, M., Rogolino, D., Bacchi, A., Rispoli, G., Fisicaro, E., Compari, C., Sechi, M., Stevaert, A., Naesens, L., 2014. Metal-chelating 2-hydroxyphenyl amide pharmacophore for inhibition of influenza virus endonuclease. Mol. Pharm. 11, 304–316.
Castilla, V., Larzabal, M., Sgalippa, N.A., Wachsman, M.B., Coto, C.E., 2005. Antiviral mode of action of a synthetic brassinosteroid against Junin virus replication. Antivir. Res. 68, 88–95.
Chen, Y.L., Tang, J., Kesler, M.J., Sham, Y.Y., Vince, R., Geraghty, R.J., Wang, Z., 2012. The design, synthesis and biological evaluations of C-6 or C-7 substituted 2-hydroxyisoquinoline-1,3-diones as inhibitors of hepatitis C virus. Bioorg. Med. Chem. 20, 467–479.
Chou, Y.Y., Cuevas, C., Carocci, M., Stubbs, S.H., Ma, M.H., Cureton, D.K., Chao, L.K., Evesson, F., He, K.M., Yang, P.L., Whelan, S.P., Ross, S.R., Kirchhausen, T., Gaudina, R., 2016. Identification and characterization of a novel broad-spectrum virus entry inhibitor. J. Virol. 90, 4494–4510.
Clegg, J.C., 2009. Influence of climate change on the incidence and impact of arenavirus diseases : a speculative assessment. Clin. Microbiol. Infect. 6, 504–509.
Cummings, M.D., Farnum, M.A., Nelen, M.I., 2006. Universal screening methods and applications of ThermoFluor. J. Biomol. Screen 11, 854–863.
Dai, D., Burgeson, J.R., Gharaibeh, D.N., Moore, A.L., Larson, R.A., Cerruti, N.R., Amberg, S.M., Bolken, T.C., Hruby, D.E., 2013. Discovery and optimization of potent broad-spectrum arenavirus inhibitors derived from benzimidazole. Bioorg. Med. Chem. Lett. 23, 744–749.
Drakulic, B.J., Stavri, M., Gibbons, S., Zizak, Z.S., Verbic, T.Z., Juranic, I.O., Zloh, M., 2009. Aryldiketo acids have antibacterial activity against MDR Staphylococcus aureus strains : structural insights based on similarity and molecular interaction fields. ChemMedChem 4, 1971–1975.
Edwards, T.C., Lomonosova, E., Patel, J.A., Li, Q., Villa, J.A., Gupta, A.K., Morrison, L.A., Bailly, F., Cotelle, P., Giannakopoulou, E., Zoidis, G., Tavis, J.E., 2017. Inhibition of hepatitis B virus replication by N-hydroxyisoquinolinediones and related polyoxygenated heterocycles. Antivir. Res. 143, 205–217.
Hastings, J.C., Selnick, H., Wolanski, B., Tomassini, J.E., 1996. Anti-influenza virus activities of 4-substituted 2,4-dioxobutanoic acid inhibitors. Antimicrob. Agents Chemother. 40, 1304–1307.
Imanishi, N., Tuji, Y., Katada, Y., Maruhashi, M., Konosu, S., Mantani, N., 2002. Additional inhibitory effect of tea extract on the growth of influenza A and B viruses in MDCK cells. Microbiol. Immunol. 46, 491–494.
Jay, M.T., Glaser, C., Fulhorst, C.F., 2005. The arenaviruses. J. Am. Vet. Med. Assoc. 227, 904–915.
Ju, H., Zhang, J., Huang, B., Kang, D., Huang, B., Liu, X., Zhan, P., 2017. Inhibitors of influenza virus polymerase acidic (PA) endonuclease: contemporary developments and perspectives. J. Med. Chem. 60, 3533–3551.
Kawasuji, T., Johns, B.A., Yoshida, H., Weatherhead, J.G., Akiyama, T., Taishi, T., Taoda, Y., Mikamiyama-Iwata, M., Murai, H., Kiyama, R., Fuji, M., Tanimoto, N., Yoshinaga, T., Seki, T., Kobayashi, M., Sato, A., Garvey, E.P., Fujiwara, T., 2013. Carbamoyl pyridone HIV-1 integrase inhibitors. 2. Bi- and tricyclic derivatives result in superior antiviral and pharmacokinetic profiles. J. Med. Chem. 56, 1124–1135.
Koshland, D.E., 1958. Application of a theory of enzyme specificity to protein synthesis. Proc. Natl. Acad. Sci. U. S. A. 44, 98–104.
Kowalinski, E., Zubieta, C., Wolkerstorfer, A., Szolar, O.H.J., Ruigrok, R.W.H., Cusack, S., 2012. Structural analysis of specific metal chelating inhibitor binding to the endonuclease domain of Influenza pH1N1 (2009) polymerase. PLoS Pathog. 8, e1002831.
Kuzuhara, T., Iwai, Y., Takahashi, H., Hatakeyama, D., Echigo, N., 2009. Green tea catechins inhibit the endonuclease activity of influenza A virus RNA polymerase. PLoS Curr. 1, RRN1052.
Larson, R.A., Dai, D., Hosack, V.T., Tan, Y., Bolken, T.C., Hruby, D.E., Amberg, S.M., 2008. Identification of a broad-spectrum arenavirus entry inhibitor. J. Virol. 82, 10768–10775.
Ling, J.X., Wei, F., Li, N., Li, J.L., Chen, L.J., Liu, Y.Y., Luo, F., Xiong, H.R., Hou, W., Yang, Z.Q., 2012. Amelioration of influenza virus-induced reactive oxygen species formation by epigallocatechin gallate derived from green tea. Acta Pharmacol. Sin. 33, 1533–1541.
Lo, M.C., Aulabaugh, A., Jin, G., Cowling, R., Bard, J., Malamas, M., Ellestad, G., 2004. Evaluation of fluorescence-based thermal shift assays for the hit identification in drug discovery. Anal. Biochem. 332, 153–159.
Martinez-Sobrido, L., De la Torre, J.C., 2017. Development of recombinant arenavirus-based vaccines. Methods Mol. Biol. 1581, 133–149.
Maurin, C., Bailly, F., Cotelle, P., 2004. Improved preparation and structural investigation of 4-aryl-4-oxo-2-hydroxy-2-butenoic acids and methyl esters. Tetrahedron 60, 6479–6486.
Maurin, C., Bailly, F., Mbemba, G., Mouscadet, J.F., Cotelle, P., 2006. Design, synthesis, and anti-integrase activity of catechol-DKA hybrids. Bioorg. Med. Chem. 14, 2978–2984.
McCormick, J.B., King, I.J., Webb, P.A., Scribner, C.L., Craven, R.B., Johnson, K.M., Elliott, L.H., Belmont-Williams, R., 1986. Lassa fever. Effective therapy with ribavirin. N. Engl. J. Med. 314, 20–26.
Mendenhall, M., Russell, A., Juelich, T., Messina, E.L., Smee, D.F., 2011a. T-705 (favipiravir) inhibition of arenavirus replication in cell culture. Antimicrob. Agents Chemother. 55, 782–787.
Mendenhall, M., Russell, A., Smee, D.F., Hall, J.O., Skirpstunas, R., Furuta, Y., Gowen, B.B., 2011b. Effective oral favipiravir (T-705) therapy initiated after the onset of clinical disease in a model of arenavirus hemorrhagic fever. PLoS Neglected Trop. Dis. 5, e1342.
Morin, B., Coutard, B., Lelke, M., Ferron, F., Kerber, R., Jamal, S., Frangeul, A., Baronti, C., Charrel, R., de Lamballerie, X., Vonrhein, C., Lescar, J., Bricogne, G., Gunther, S., Canard, B., 2010. The N-terminal domain of the arenavirus L protein is an RNA endonuclease essential in mRNA transcription. PLoS Pathog. 6, e1001038.
Nakayama, M., Suzuki, K., Toda, M., Okubo, S., Hara, Y., Shimamura, T., 1993. Inhibition of the infectivity of influenza virus by tea polyphenols. Antivir. Res. 21, 289–299.
Nakazawa, M., Kadowaki, S.E., Watanabe, I., Kadowaki, Y., Takei, M., Fukuda, H., 2008. PA subunit of RNA polymerase as a promising target for anti-influenza virus agents. Antivir. Res. 78, 194–201.
Ngo, N., Henthorn, K.S., Cisneros, M.I., Cubitt, B., Iwasaki, M., de la Torre, J.C., Lama, J., 2016. Identification and mechanism of action of a novel small-molecule inhibitor of arenavirus multiplication (vol 89, pg 10924, 2015). J. Virol. 90 8381-8381.
Niesens, F.H., Berglund, H., Vedadi, M., 2007. The use of differential scanning fluorimetry to detect ligand interactions that promote protein stability. Nat. Protoc. 2, 2212–2221.
Omoto, S., Speranzini, V., Hashimoto, T., Noshi, T., Yamaguchi, H., Kawai, M., Kawaguchi, K., Uehara, T., Shishido, T., Naito, A., Cusack, S., 2018. Characterization of influenza virus variants induced by treatment with the endonuclease inhibitor baloxavir marboxil. Sci. Rep. 8, 9633.
Ortiz-Riano, E., Ngo, N., Devito, S., Eggink, D., Munger, J., Shaw, M.L., de la Torre, J.C., Martinez-Sobrido, L., 2014. Inhibition of arenavirus by A3, a pyrimidine biosynthesis inhibitor. J. Virol. 88, 878–889.
Pantoliano, M.W., Petrella, E.C., Kwasnoski, J.D., Lobanov, V.S., Myslik, J., Graf, E., Carver, T., Asel, E., Springer, B.A., Lane, P., Salemme, F.R., 2001. high-density miniaturized thermal shift assays as a general strategy for drug discovery. J. Biomol. Screen 6, 429–440.
Parkes, K.E., Ermert, P., Fassler, J., Ives, J., Martin, J.A., Merrett, J.H., Obrecht, D., Williams, G., Klumpp, K., 2003. Use of a pharmacophore model to discover a new class of influenza endonuclease inhibitors. J. Med. Chem. 46, 1153–1164.
Pasquato, A., Kunz, S., 2016. Novel drug discovery approaches for treating arenavirus infections. Expert Opin. Drug Discov. 11, 383–393.
Pasquato, A., Rochat, C., Burri, D.J., Pasqual, G., de la Torre, J.C., Kunz, S., 2012. Evaluation of the anti-arenaviral activity of the subtilisin kexin isozyme-1/site-1 protease inhibitor PF-429242. Virology 423, 14–22.
Patil, S., Kamath, S., Sanchez, T., Neamiti, N., Schinazic, R.F., Buolamwinia, J.K., 2007. Synthesis and biological evaluation of novel 5(H)-phenanthridin-6-ones, 5(H)-phenanthridin-6-one diketo acid and polycyclic aromatic diketo acid analogs as new HIV-1 integrase inhibitors. Bioorg. Med. Chem. 15, 1212–1228.
Polyak, S.J., Zheng, S., Harnish, D.G., 1995a. 5′ termini of Pichinde arenavirus S RNAs and mRNAs contain nontemplated nucleotides. J. Virol. 69, 3211–3215.
Polyak, S.J., Zheng, S., Harnish, D.G., 1995b. Analysis of Pichinde arenavirus transcription and replication in human THP-1 monocytic cells. Virus Res. 36, 37–48.
Priet, S., Roux, L., Saez-Ayala, M., Ferron, F., Canard, B., Alvarez, K., 2015. Enzymatic synthesis of acyclic nucleoside thiophosphonate diphosphates: effect of the alpha-phosphorus configuration on HIV-1 RT activity. Antivir. Res. 117, 122–131.
Reguera, J., Gerlach, P., Rosenthal, M., Gaudon, S., Coscia, F., Gunther, S., Cusack, S.,

2016. Comparative structural and functional analysis of Bunyavirus and Arenavirus cap-snatching endonucleases. PLoS Pathog. 12, e1005636.
Reguera, J., Weber, F., Cusack, S., 2010. Bunyaviridae RNA polymerases (L-protein) have an N-terminal, Influenza-like endonuclease domain, essential for viral cap-dependent transcription. PLoS Pathog. 6, e1001101.
Reynard, S., Russier, M., Fizer, A., Carnec, X., Baize, S., 2014. Exonuclease domain of the Lassa virus nucleoprotein is critical to avoid RIG-I signaling and to inhibit the innate immune response. J. Virol. 88 (23), 13923–13927.
Rogolino, D., Carcelli, M., Sechi, M., Neamati, N., 2012. Viral enzymes containing magnesium : metal Binding as a successful strategy in drug design. Coord. Chem. Rev. 256, 3063–3086.
Saez-Ayala, M., Laban Yekwa, E., Carcelli, M., Canard, B., Alvarez, K., Ferron, F., 2018. Crystal structures of LCMV endonuclease domain complexed with diketo acid ligands. IUCrJ 5, LZ5019.
Sechi, M., Bacchi, A., Carcelli, M., Compari, C., Duce, E., Fisicaro, E., Rogolino, D., Gates, P., Derudas, M., Al-Mawsawi, L.Q., Neamati, N., 2006. From ligand to complexes: inhibition of human immunodeficiency virus type 1 integrase by beta-diketo acid metal complexes. J. Med. Chem. 49, 4248–4260.
Sepulveda, C.S., Fascio, M.L., Mazzucco, M.B., Palacios, M.L., Pellon, R.F., Garcia, C.C., D'Accorso, N.B., Damonte, E.B., 2008. Synthesis and evaluation of N-substituted acridones as antiviral agents against haemorrhagic fever viruses. Antivir. Chem. Chemother. 19, 41–47.
Sepulveda, C.S., Garcia, C.C., Damonte, E.B., 2018. Antiviral activity of A771726, the active metabolite of leflunomide, against Junin virus. J. Med. Virol. 90 (5), 819–827.
Sepulveda, C.S., Garcia, C.C., Fascio, M.L., D'Accorso, N.B., Palacios, M.L.D., Pellon, R.F., Damonte, E.B., 2012. Inhibition of Junin virus RNA synthesis by an antiviral acridone derivative. Antivir. Res. 93, 16–22.
Song, J.M., Lee, K.H., Seong, B.L., 2005. Antiviral effect of catechins in green tea on influenza virus. Antivir. Res. 68, 66–74.
Song, M.S., Kumar, G., Shadrick, W.R., Zhou, W., Jeevan, T., Li, Z., Slavish, P.J., Fabrizio, T.P., Yoon, S.W., Webb, T.R., Webby, R.J., White, S.W., 2016. Identification and characterization of influenza variants resistant to a viral endonuclease inhibitor. Proc. Natl. Acad. Sci. U. S. A. 113, 3669–3674.
Steinmann, J., Buer, J., Pietschmann, T., Steinmann, E.,F., 2013. anti-infective properties of epigallocatechin-3-gallate (EGCG), a component of green tea. Br. J. Pharmacol. 168, 1059–1073.
Stevaert, A., Dallochio, R., Dessi, A., Pala, N., Rogolino, D., Sechi, M., Naesens, L., 2013. Mutational analysis of the binding pockets of the diketo acid inhibitor L-742,001 in the influenza virus PA endonuclease. J. Virol. 87, 10524–10538.
Stevaert, A., Nurra, S., Pala, N., Carcelli, M., Rogolino, D., Shepard, C., Domaoal, R.A., Kim, B., Alfonso-Prieto, M., Marras, S.A.E., Sechi, M., Naesens, L., 2015. An integrated biological approach to guide the development of metal-chelating inhibitors of Influenza virus PA endonuclease. Mol. Pharmacol. 87, 323–337.
Suchaud, V., Bailly, F., Lion, C., Calmels, C., Andreola, M.L., Christ, F., Debyser, Z., Cotelle, P., 2014. Investigation of a novel series of 2-hydroxyisoquinoline-1,3(2H,4H)-diones as human immunodeficiency virus type 1 integrase inhibitors. J. Med. Chem. 57, 4640–4660.
Summa, V., Petrocchi, A., Bonelli, F., Crescenzi, B., Donghi, M., Ferrara, M., Fiore, F., Gardelli, C., Gonzalez Paz, O., Hazuda, D.J., Jones, P., Kinzel, O., Laufer, R., Monteagudo, E., Muraglia, E., Nizi, E., Orvieto, F., Pace, P., Pescatore, G., Scarpelli, R., Stillmock, K., Witmer, M.V., Rowley, M., 2008. Discovery of raltegravir, a potent, selective orally bioavailable HIV-integrase inhibitor for the treatment of HIV-AIDS infection. J. Med. Chem. 51, 5843–5855.
Tomassini, J., Selnick, H., Davies, M.E., Armstrong, M.E., Baldwin, J., Bourgeois, M., Hastings, J., Hazuda, D., Lewis, J., McClements, W., 1994. Inhibition of cap (m7GpppXm)-dependent endonuclease of influenza virus by 4-substituted 2, 4-dioxobutanoic acid compounds. Antimicrob. Agents Chemother. 38, 2827–2837.
Tomassini, J.E., Davies, M.E., Hastings, J.C., Lingham, R., Mojena, M., Raghoobar, S.L., Singh, S.B., Tkacz, J.S., Goetz, M.A., 1996. A novel antiviral agent which inhibits the endonuclease of influenza viruses. Antimicrob. Agents Chemother. 40, 1189–1193.
Uckun, F.M., Venkatachalam, T.K., Erbeck, D., Chen, C.L., Petkevich, A.S., Vassilev, A., 2005. Zidampidine, an aryl phosphate derivative of AZT: in vivo pharmacokinetics, metabolism, toxicity, and anti-viral efficacy against hemorrhagic fever caused by Lassa virus. Bioorg. Med. Chem. 13, 3279–3288.
Verbic, T., Drakulic, B., Zloh, M., Pecelj, J., Popovic, G., Juranic, I., 2007. An LFER study of the protolytic equilibria of 4-aryl-2,4-dioxobutanoic acids in aqueous solutions. J. Serb. Chem. Soc. 72, 1201–1216.
Xu, Y.-S., Zeng, C.-C., Li, X.-M., Zhong, R.-G., Zeng, Y., 2006. Design, synthesis and Cu2+ recognition of β-diketoacid and quinoxalone derivatives bearing caffeoyl or galloyl moieties linked by arylamide as potential HIV integrase inhibitors. Chin. J. Chem. 24, 1086–1094.